Coexistence of the (23 × √3) Au(111) Reconstruction and a Striped Phase Self-Assembled Monolayer

S. B. Darling, A. W. Rosenbaum, Yi Wang, and S. J. Sibener*

The James Franck Institute and Department of Chemistry, The University of Chicago, 5640 South Ellis Ave., Chicago, Illinois 60637

Received April 8, 2002. In Final Form: June 24, 2002

We have studied the effect of adsorption of a low-density alkanethiol monolayer on the state of the Au(111) reconstruction. It is commonly believed that the substrate deconstructs following formation of a thiolate self-assembled monolayer, but our results suggest this is not always the case. Helium diffraction from 1-decanethiol and 1-octanethiol striped phase monolayers is exploited to establish the surface nearest-neighbor spacing and to illustrate a unit cell corresponding to the long dimension of the (23 × √3) reconstruction. Using our observed 0.198 Å^{-1} peak spacing and the (11.5 × √3) unit cell reported in the literature, we measure a substrate nearest-neighbor spacing of 2.76 Å along the [1$\bar{1}$0] direction, which represents the atomic spacing of the uniaxially compressed, reconstructed gold surface. Moreover, $^1/_2$-order peaks in the diffraction from decanethiol/Au(111) demonstrate a distinction between neighboring thiolate dimers. These peaks are not observed for the octanethiol/Au(111) system. Therefore, the $^1/_2$-order peaks are not an inherent characteristic of alkanethiol SAMs. The most likely explanation for these peaks is a reconstructed substrate. Complementary scanning tunneling microscopy data are also presented that show persistence of the reconstruction during growth of a decanethiol striped phase monolayer and no evidence for vacancy islands typically associated with deconstruction or alternate reconstructions. Our model involving a still-reconstructed substrate is consistent with all of the available data, while alternative models fail to explain the results presented in this article.

Introduction

Self-assembled monolayers (SAMs) based on a sulfur headgroup have been widely studied using numerous surface analysis techniques, inspired by both fundamental studies of self-organization and potential technological applications. Despite this extensive scrutiny, the structure of the adsorbed species and the details of the interfacial region are still a topic of controversy.[1−5] Many groups have investigated the nature of the interface between the standing *c*(4 × 2) phase of 1-decanethiol (C10) and the Au(111) surface. Conclusions based on these studies have often been extrapolated to describe the analogous interface for the lower density pinstripe phase. It is our contention that this extrapolation is inappropriate, leading in some instances to erroneous structural conclusions.

Unlike other fcc metal close-packed (111) surfaces, the Au(111) surface undergoes a reconstruction when clean. Various real- and reciprocal-space experimental techniques, complemented by theoretical studies, have been used to examine this surprisingly complex structure.[6−15] Early low-energy electron diffraction (LEED) studies produced several models for the structure of the reconstruction,[6,7] from which a model invoking a uniform uniaxial contraction of the topmost layer leading to a rectangular (23 × √3) unit cell emerged. Transmission electron microscopy (TEM) experiments expanded on this model by proposing a stacking fault structure in which there are alternating fcc- and hcp-type stacking regions within the unit cell.[8] Helium diffraction corroborated the stacking fault structure and suggested that the fcc−hcp transition regions were best modeled with Frenkel−Kontorova solitons;[11] however, a theoretical approach incorporating a double-sine Gordon potential provides a more natural description.[15]

Scanning tunneling microscopy (STM) studies finally put an end to this issue with direct atomic-scale observations of the reconstruction.[13,14] These experiments confirmed the stacking fault domain structure and verified the uniform uniaxial contraction in the [1$\bar{1}$0] direction. Lateral displacement of 0.9 Å in the [11$\bar{2}$] direction within the unit cell agreed well with shifting from fcc to hcp stacking. Figure 1 schematically depicts a unit cell of the reconstructed surface. In addition, Barth et al. reported a long-range superstructure created by a correlated periodic bending of the parallel reconstruction corrugation lines by ±120° every 250 Å.[14] This superstructure is the root of the designations "herringbone" and "chevron" for the gold reconstruction. Such extended structure suggests large-scale elastic lattice strain and indicates an overall propensity for isotropic contraction. Also, these STM studies revealed that surface steps are crossed by the

* To whom correspondence should be addressed: phone 773-702-7193; Fax 773-702-5863; e-mail s-sibener@uchicago.edu.

(1) Dubois, L. H.; Nuzzo, R. G. *Annu. Rev. Phys. Chem.* **1992**, *43*, 437.
(2) Yeganeh, M. S.; Dougal, S. M.; Polizzotti, R. S.; Rabinowitz, P. *Phys. Rev. Lett.* **1995**, *74*, 1811.
(3) Fenter, P.; Schreiber, F.; Berman, L.; Scoles, G.; Eisenberger, P.; Bedzyk, M. J. *Surf. Sci.* **1998**, *412/413*, 213.
(4) Kluth, G. J.; Carraro, C.; Maboudian, R. *Phys. Rev. B* **1999**, *59*, 10449.
(5) Wang, Y. W.; Fan, L. J. *Langmuir* **2002**, *18*, 1157.
(6) Perdereau, J.; Biberian, J. P.; Rhead, G. E. *J. Phys. F* **1974**, *4*, 798.
(7) Hove, M. A. v.; Koestner, R. J.; Stair, P. C.; Bibérian, J. P.; Kesmodel, L. L.; Bartoš, I.; Somorjai, G. A. *Surf. Sci.* **1981**, *103*, 189.
(8) Heyraud, J. C.; Métois, J. J. *Surf. Sci.* **1980**, *100*, 519.
(9) Tanishiro, Y.; Kanamori, H.; Takayanagi, K.; Yagi, K.; Honjo, G. *Surf. Sci.* **1981**, *111*, 395.
(10) Marks, L. D.; Heine, V.; Smith, D. J. *Phys. Rev. Lett.* **1984**, *52*, 656.
(11) Harten, U.; Lahee, A. M.; Toennies, J. P.; Wöll, C. *Phys. Rev. Lett.* **1985**, *54*, 2619.
(12) Bach, C. E.; Giesen, M.; Ibach, H.; Einstein, T. L. *Phys. Rev. Lett.* **1997**, *78*, 4225.
(13) Wöll, C.; Chiang, S.; Wilson, R. J.; Lippel, P. H. *Phys. Rev. B* **1989**, *39*, 7988.
(14) Barth, J. V.; Brune, H.; Ertl, G.; Behm, R. J. *Phys. Rev. B* **1990**, *42*, 9307.
(15) El-Batanouny, M.; Burdick, S.; Martini, K. M.; Stancioff, P. *Phys. Rev. Lett.* **1987**, *58*, 2762−2765.

10.1021/la020334x CCC: $22.00
Published on Web 08/22/2002

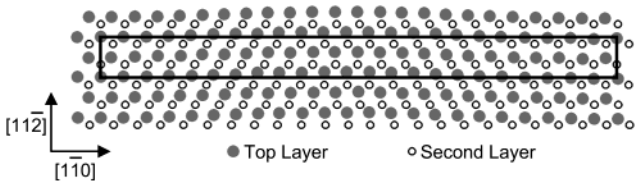

Figure 1. Top view schematic of the Au(111) reconstruction. Solid circles are the top layer, and open circles are the second layer. The topmost layer is compressed by 4.4% along the ⟨1$\bar{1}$0⟩ azimuth, leading to a smooth and periodic variation in the registry with the second layer from ABC to ABA to ABC stacking. This compression creates an enhanced charge density corrugation easily detected by surface-sensitive helium diffraction.

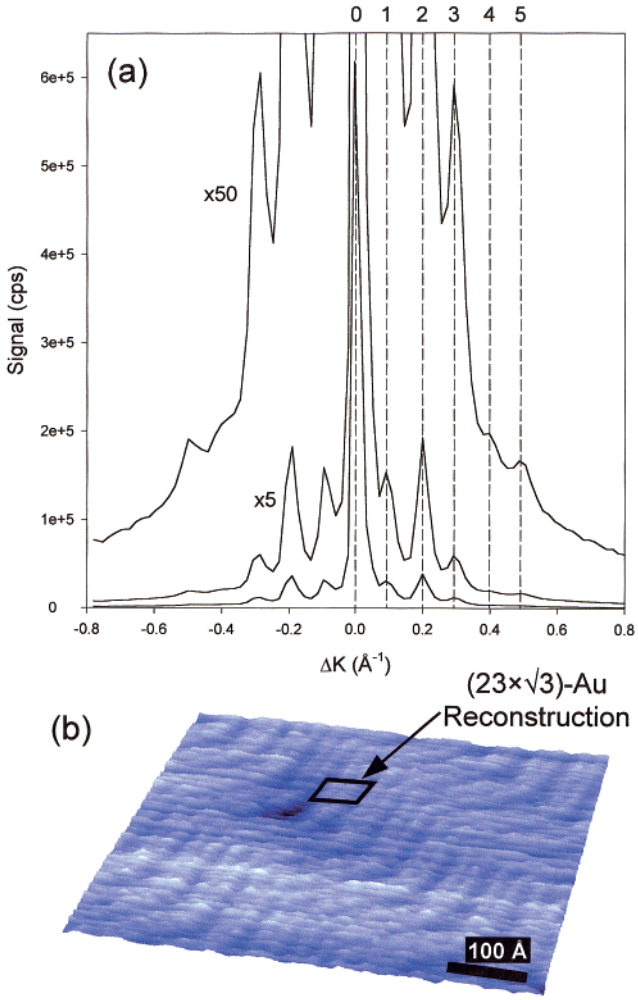

Figure 2. (a) Helium diffraction scan of the (23 × √3) reconstruction of Au(111) in the ⟨1$\bar{1}$0⟩ direction. Five orders of diffraction are observed on both sides of specular. Kinematic conditions: $E_i = 19.4$ meV, $\theta_i = 28.4°$, $T_{crystal} = 200$ K. (b) 600 Å × 600 Å UHV-STM image of Au(111) (23 × √3) and herringbone reconstructions. Experimental conditions: 1 nA tunneling current, 600 mV positive bias with respect to the tip, 298 K surface. The box denotes the (23 × √3) unit cell schematized in Figure 1.

reconstruction with full correlation in phase and orientation, indicating persistence due to interaction across the step edge. Helium diffraction showing the (23 × √3) unit cell is depicted in Figure 2a, and an image of the herringbone reconstruction taken with our UHV-STM is shown in Figure 2b.

With the structure well understood, studies were undertaken to test the stability of the gold reconstruction under various environmental changes including temperature, electric potential, and exposure to assorted adsorbates. Using X-ray diffraction, the long-range herringbone superstructure is found to deconstruct starting at 865 K, while the smaller (23 × √3) reconstruction is stable until 1250 K.[16,17] In an electrochemical environment, however, one can stabilize the deconstructed (111) surface with positive potentials (≥0.2 V) at room temperature.[18] This result suggests that the existence of the reconstruction relies on excess negative surface charge density. One can test this notion using adsorbates with varying electronegativity; those with higher electron affinity than gold should withdraw charge from the surface and deconstruct the compression of the top layer while those with lower electron affinity should not affect the reconstruction. Indeed, it has been shown using X-ray diffraction and optical second harmonic generation (SHG) that when (electronegative) halides or sulfur atoms adsorb on the Au(111) surface, they globally lift the reconstruction,[19−21] while adsorption of (electropositive) sodium atoms leaves the reconstruction intact until exposure is sufficient to induce surface alloying.[22]

Moving beyond simple adsorbates to alkanethiols, Yeganeh et al. performed infrared−visible sum-frequency generation (SFG) experiments to probe the interfacial structure of a C18 SAM.[2] According to this study, the (23 × √3) reconstruction reverts to (1 × 1) symmetry upon adsorption of the standing phase SAM. As the thiolate headgroups of the C18 molecules are relatively electronegative and the molecular density is substantial, this outcome is not unexpected. Given this result, it has been generally assumed that the reconstruction is lifted upon initial chemisorption of thiols. Recent STM work by Dishner et al. using methanethiol/Au(111), however, clearly illustrates that not only can the reconstruction persist after thiol adsorption, but it can also influence the resulting SAM structure,[23] much as it does with *n*-alkane SAMs.[24] Limitations inherent to STM preclude direct imaging of the underlying substrate, but domains of the monolayer often track the herringbone geometry. Optical SHG studies of *β*-mercaptocarboxylic acid SAMs on Au(111) provide direct evidence for the persistence of the substrate reconstruction despite the presence of a dense thiolate monolayer.[25]

Absent from this discussion has been the effect of lower coverage adsorbates on the gold reconstruction. Among the most significant of these monolayers is the lying-down, striped phase of decanethiol. Ideal coverage for this phase is $\theta = 0.27$ ML compared to $\theta = 0.47$ ML for the dense standing phase. A lower coverage translates to fewer electronegative sulfur headgroups and, hence, to ambiguity as to the fate of the electron-hungry reconstruction. Data in the literature, though circumstantial, are com-

(16) Huang, K. G.; Gibbs, D.; Zehner, D. M.; Sandy, A. R.; Mochrie, S. G. J. *Phys. Rev. Lett.* **1990**, *65*, 3313.
(17) Sandy, A. R.; Mochrie, S. G. J.; Zehner, D. M.; Huang, K. G.; Gibbs, D. *Phys. Rev. B* **1991**, *43*, 4667.
(18) Etgens, V. H.; Alves, M. C. M.; Tadjeddine, A. *Electrochim. Acta* **1999**, *45*, 591.
(19) Wang, J.; Ocko, B. M.; Davenport, A. J.; Isaacs, H. S. *Phys. Rev. B* **1992**, *46*, 10321.
(20) Friedrich, A.; Shannon, C.; Pettinger, B. *Surf. Sci.* **1990**, *251/252*, 587.
(21) Andreasan, G.; Vericat, C.; Vela, M. E.; Salvarezza, R. C. *J. Chem. Phys.* **1999**, *111*, 9457.
(22) Barth, J. V.; Behm, R. J.; Ertl, G. *Surf. Sci.* **1995**, *341*, 62.
(23) Dishner, M. H.; Hemminger, J. C.; Feher, F. J. *Langmuir* **1997**, *13*, 2318.
(24) Xie, Z. X.; Xu, X.; Tang, J.; Mao, B. W. *J. Phys. Chem. B* **2000**, *104*, 11719.
(25) Baba, R.; Fujishima, A.; Hashimoto, K.; Miwa, T. *MCLC S&T, Sect. B* **1999**, *22*, 497.

pelling. STM experiments performed by Poirier involving partial coverage images of the striped phase exhibit unmistakable substrate reconstruction in those areas not concealed by the SAM.[26−28] Moreover, the extant SAM domains track the herringbone contour while the visible reconstructed domains are most likely covered with a lattice gas of thiols. In another study, Fitts et al. have proposed that the gold reconstruction is destroyed during adsorption of striped phase thiolate SAMs.[29] Deconstruction, however, should be accompanied by vacancy island formation to accommodate the ejection of excess Au atoms.[27] Vacancy island formation may also be ascribed to creation of auxiliary reconstructions. Fitts et al. do not observe these vacancy islands during growth of the striped phase, suggesting that the original reconstruction survived formation of the SAM. They propose a previously unobserved rippling of gold atoms to accommodate the excess atoms ejected during deconstruction. Our model described below, however, explains both these real-space observations and our new reciprocal-space results while avoiding the need for novel effects. Indeed, at exposures comparable to those used in our study, Eberhardt has proposed on the basis of X-ray diffraction that the surface will still be largely reconstructed;[30] unpublished results suggest the situation may be more complicated.[31]

Taken together, these findings raise doubts about the common view that all thiol SAMs deconstruct the gold substrate. If the substrate is indeed still reconstructed underneath a striped phase SAM, it will have consequences for the structure of the monolayer as well. Before discussing evidence for this effect, it is necessary to appreciate the subtleties within the structure of the striped phase.

Despite the extensive array of experiments aimed at deciphering the structure of 1-decanethiol SAMs, there is still some dispute as to the precise structure of these systems. In this article, we focus on the low-coverage striped phase. With few exceptions, the striped phase structure debate is between two unit cells: $(11.5 \times \sqrt{3})$ and $(11 \times \sqrt{3})$. Camillone et al. have reported a rectangular $(11 \times \sqrt{3})$ unit cell based on helium diffraction spectra.[32] Their conclusion is based on an experimentally observed peak spacing of $\Delta K = 0.198$ Å^{-1} along the $\langle 1\bar{1}0 \rangle$ azimuth and the Au(111) nearest-neighbor spacing of 2.884 Å:

$$\frac{2\pi}{11 \times 2.884\ \text{Å}} = 0.198\ \text{Å}^{-1} \qquad (1)$$

Clearly, this conclusion implicitly requires that the substrate be *deconstructed*, as has been commonly assumed. There is, however, an alternate interpretation of the observed peak spacing. Interestingly, using the compressed atomic spacing appropriate for the $(23 \times \sqrt{3})$ *reconstructed* surface (2.758 Å), the same peak-to-peak distance suggests an $(11.5 \times \sqrt{3})$ unit cell:

$$\frac{2\pi}{11.5 \times 2.758\ \text{Å}} = 0.198\ \text{Å}^{-1} \qquad (2)$$

LEED and STM data also both point conclusively to a primitive $(11.5 \times \sqrt{3})$ unit cell (identified as $c(23 \times \sqrt{3})$) for the pinstripe phase.[33−35] One of these studies specifically demonstrates a shift of the corrugation pattern of adjacent stripe pairs that corresponds to exactly half of the Au(111) next-nearest-neighbor distance (4.995 Å).[35] Therefore, the stripe periodicity must be $(n + {}^1/_2)$ of the gold nearest-neighbor spacing, ruling out an integer unit cell such as $(11 \times \sqrt{3})$. This seemingly subtle distinction has potentially significant ramifications for both the structure of the archetypal SAM and the structure of the substrate below. In this article, we present new real- and reciprocal-space data that show the Au(111) reconstruction survives adsorption of a low-density alkanethiol SAM.

Experimental Section

The majority of these experiments were carried out in a high-momentum and energy-resolution helium atom scattering apparatus. This instrument has been described in detail elsewhere,[36,37] and the design will only be summarized here. It consists of a supersonic helium beam source, an UHV scattering chamber equipped with appropriate surface characterization tools, and a rotating, long flight path (crystal-to-ionizer distance of 1.005 m) quadrupole mass spectrometer based detector. The angular collimation yields a resolution of 0.22°. The Au(111) crystal used in these studies was cleaned by repeated cycles of sputtering with 0.5 keV Ne^+ ions followed by annealing above 1000 K until contaminant levels were below our Auger detection limit, and helium reflectivity was maximized. Surface crystallinity was confirmed by high-quality helium diffraction from the $(23 \times \sqrt{3})$ herringbone reconstruction showing an unusually robust five Bragg orders of diffraction with a concomitant low level of diffuse background (Figure 2). The average domain size, extracted from the FWHM of the specular diffraction peak with the instrument function deconvoluted, is ≥400 Å.

The 1-decanethiol (Aldrich, 97%) was purified by repeated freeze−pump−thaw cycles and dosed to scattering chamber backfill pressures of approximately 10^{-7} Torr via a stainless steel tube directed at the gold surface. This directed doser, situated ∼1 cm from the surface, delivers a higher effective local pressure at the target surface and is employed for vapor phase deposition of organics. High-quality SAMs with domain sizes as large as the underlying gold terraces were prepared by dosing at a surface temperature of 280 K followed by a 10 min anneal near the desorption temperature ($T_{\text{anneal}} = 380$ K) except where noted. Diffraction from the SAMs was obtained at 80 K to optimize the signal-to-noise ratio of the elastic diffraction by minimizing Debye−Waller attenuation. All data were recorded by scattering along the $\langle 1\bar{1}0 \rangle$ azimuth.

STM experiments were performed in a stainless steel UHV chamber with a base pressure of 5.5×10^{-11} Torr equipped with an Omicron Micro-STM adapted by us for elevated temperature imaging and standard sample cleaning and characterization tools. Details of the design of the proximity heater and the UHV-STM system are given elsewhere.[38] Experimental images were recorded at room temperature in constant current mode with the tip biased +600 mV with respect to the sample and 1 nA tunneling current. Dosing was performed by backfilling the chamber with 1-decanethiol, prepared as described above, using a high-precision leak valve located near the STM. Sample preparation involved

(26) Poirier, G. E.; Plyant, E. D. *Science* **1996**, *272*, 1145.
(27) Poirier, G. E. *Langmuir* **1997**, *13*, 2019.
(28) Poirier, G. E.; Fitts, W. P.; White, J. M. *Langmuir* **2001**, *17*, 1176.
(29) Fitts, W. P.; White, J. M.; Poirier, G. E. *Langmuir* **2002**, *18*, 1561.
(30) Eberhardt, A. Ph.D. Thesis, Princeton University, 1997; pp 128−136.
(31) Fenter, P. Private communication.
(32) Camillone, N.; Leung, T. Y. B.; Schwartz, P.; Eisenberger, P.; Scoles, G. *Langmuir* **1996**, *12*, 2737. Following high-temperature anneals, Camillone et al. observed a unit cell expansion similar to that depicted in Figure 7. The authors denote the expanded unit cell as $(11.5 \times \sqrt{3})$ with respect to a *deconstructed* substrate. This should not be confused with the $(11.5 \times \sqrt{3})$ assignment described in the current paper that refers to registry with a $(23 \times \sqrt{3})$ *reconstructed* substrate.
(33) Gerlach, R.; Polanski, G.; Rubahn, H.-G. *Appl. Phys. A: Mater. Sci. Process.* **1997**, *65*, 375.
(34) Poirier, G. E. *Langmuir* **1999**, *15*, 1167.
(35) Staub, R.; Toerker, M.; Fritz, T.; Schmitz-Hübsch, T.; Sellam, F.; Leo, K. *Langmuir* **1998**, *14*, 6693.
(36) Gans, B.; King, S. F.; Knipp, P. A.; Koleske, D. D.; Sibener, S. J. *Surf. Sci.* **1992**, *264*, 81.
(37) Niu, L.; Koleske, D. D.; Gaspar, D. J.; Sibener, S. J. *J. Chem. Phys.* **1995**, *102*, 9077.
(38) Pearl, T. P.; Sibener, S. J. *Rev. Sci. Instrum.* **2000**, *71*, 124.

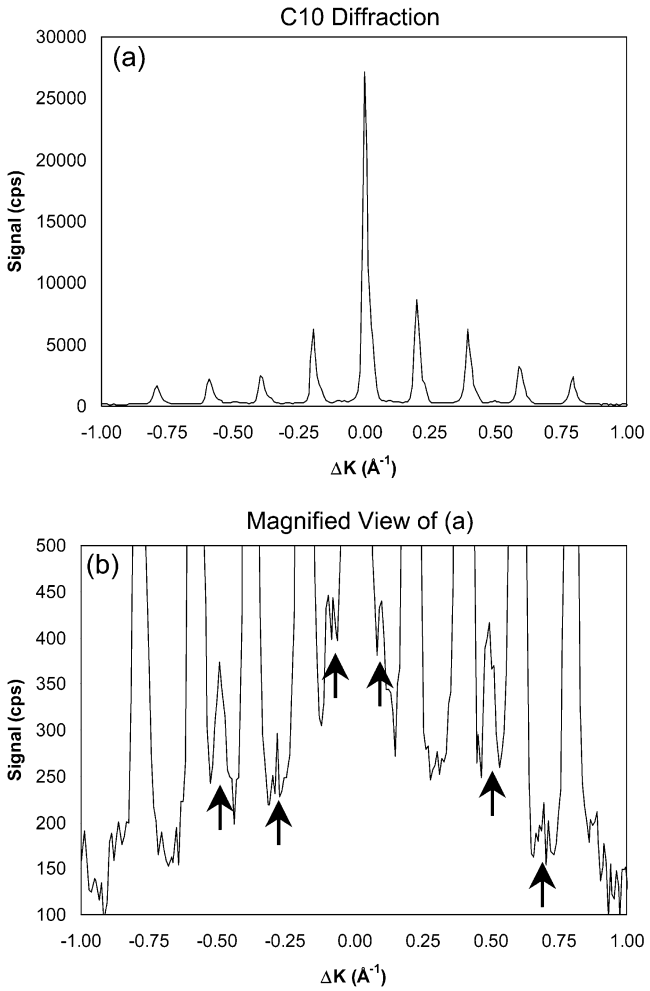

Figure 3. (a) Helium diffraction scan of one of the three equivalent domains of the (11.5 × √3) striped phase of 1-decanethiol on Au(111) in the ⟨1$\bar{1}$0⟩ direction. The other two domains are structurally identical and rotated ±120° from this domain. Four orders of diffraction are observed on both sides of specular. Kinematic conditions: $E_i = 16.6$ meV, $\theta_i = 31.0°$, $T_{crystal} = 80$ K. (b) A zoomed-in view of the spectrum shown in (a). Arrows highlight the positions of the $^1/_2$-order peaks with three visible on each side of specular.

cycles of 1 keV Ar^+ sputtering between 300 and 1100 K and annealing by electron bombardment at 1100 K. Surface cleanliness was checked by Auger electron spectroscopy, and crystallinity was verified using LEED and STM.

Results and Discussion

A characteristic diffraction scan of the chemisorbed, low-density striped phase of C10/Au(111) obtained via a ~20 langmuir dose at the target is shown in Figure 3. An average domain size of at least 400 Å is inferred from the width of the diffraction peaks because there is no broadening added to the substrate specular peak width. The peak-to-peak spacing in this spectrum is 0.198 $Å^{-1}$, which agrees with previously published helium diffraction from this system.[32,39] As described above, this spacing alone is not sufficient to distinguish between an (11 × √3) and an (11.5 × √3) unit cell because the atomic spacing in the topmost layer of the substrate, which serves as the reference for the overlayer nomenclature, is not probed. However, LEED and STM studies have clearly demonstrated that the C10 striped phase forms a p(11.5 × √3) structure.[33−35] Assuming this conclusion to be true, therefore, the 0.198 $Å^{-1}$ peak spacing in the helium diffraction proves that the substrate nearest-neighbor spacing must be 2.76 Å (see eq 2). The nearest-neighbor spacing for Au(111) is 2.88 Å while the Au(23 × √3) spacing is 2.76 Å. Thus, our helium diffraction data considered in the context of the available LEED and STM data prove that the gold is reconstructed underneath the striped phase SAM.

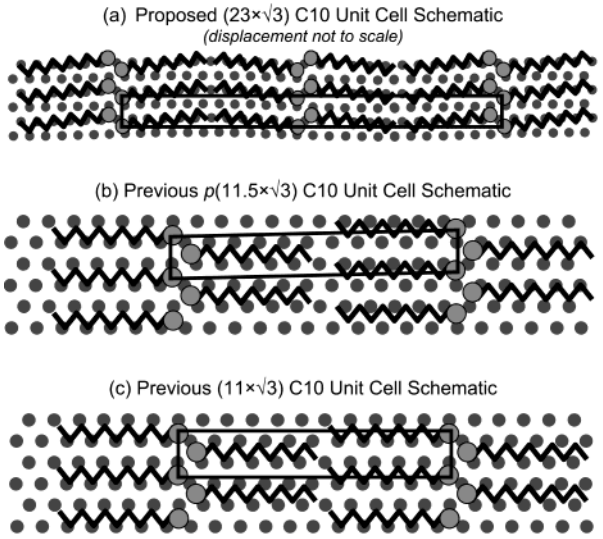

Figure 4. (a) Exaggerated schematic of the proposed structure of the (11.5 × √3) striped phase of 1-decanethiol on the reconstructed Au(111) surface. The box represents the overlayer unit cell. (b) and (c) are previously proposed structures for the C10 striped phase. (a) and (b) only differ in that the substrate is reconstructed in (a) while (c) involves a qualitatively different structure for the SAM in that the long-dimension registry is 11 rather than 11.5 nearest-neighbor spacings.

Looking closer at these data, moreover, reveals additional, smaller peaks centered between the principals (Figure 3b). This phenomenon was also observed by Schwartz.[40] These $^1/_2$-order peaks can only arise from periodicity on a scale exactly twice that of the C10 dimer, namely, 63.4 Å. Interestingly, and we will argue not coincidentally, this distance is identical to the long dimension of the Au(23 × √3) reconstruction unit cell. Figure 4 depicts a proposed schematic structure of the C10 pinstripe phase adsorbed on a still-reconstructed Au(111) surface. Displacement along the [11$\bar{2}$] direction has been exaggerated to clarify the nonlinear structure composed of four decanethiol molecules. If it were not for the fortuitous match between the length of the (23 × √3) reconstruction unit cell and the length of two (11.5 × √3) C10 repeat units, the $^1/_2$-order peaks would be imperceptible. A second possible explanation for the additional peaks is an as yet unobserved, long-range periodic structural differentiation between alternating thiol dimers adsorbed on deconstructed gold.

To test these competing theories, we studied a chemically analogous striped phase with a different molecular length, effectively removing the unit cell size correspondence present between C10 and Au(23 × √3). 1-Octanethiol (C8), known to form a (10 × √3) unit cell,[41] is chemically very similar to C10 and has a vapor pressure well-suited to gas phase dosing, and yet the Au(111) reconstruction cannot accommodate an integer number

(39) Darling, S. B.; Rosenbaum, A. W.; Sibener, S. J. *Surf. Sci.* **2001**, *478*, L313.

(40) Schwartz, P. V. Ph.D. Thesis, Princeton University, 1998.

(41) Kobayashi, K.; Yamada, H.; Horiuchi, T.; Matsushige, K. *Jpn. J. Appl. Phys.* **1998**, *37*, 6183.

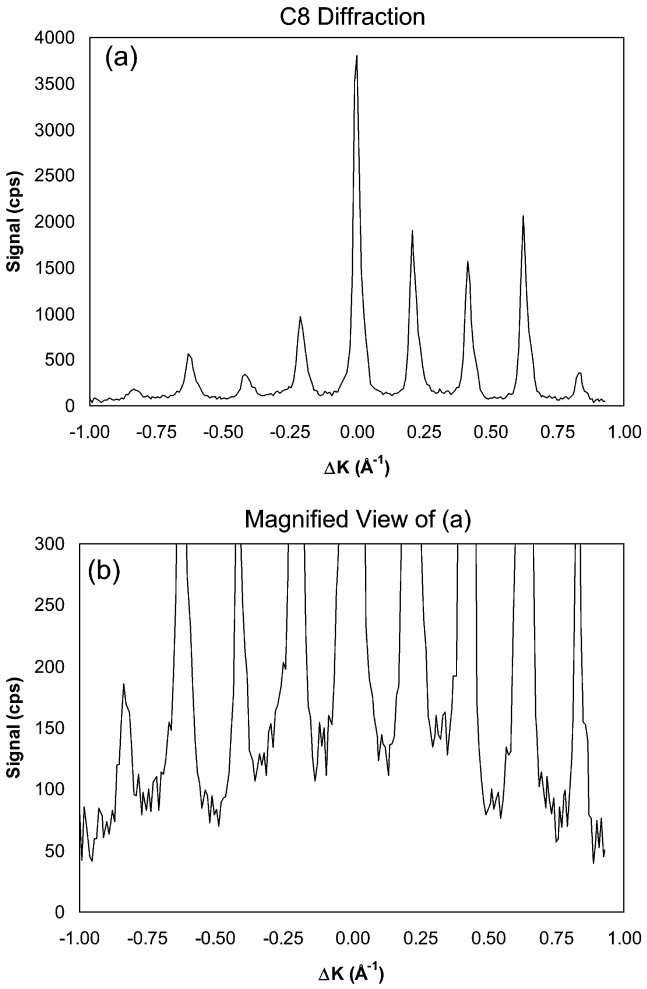

Figure 5. (a) Helium diffraction scan of one of the three equivalent domains of the striped phase of 1-octanethiol on Au(111) in the ⟨1$\bar{1}$0⟩ direction. The other two domains are structurally identical and rotated ±120° from this domain. Four orders of diffraction are observed on both sides of specular. Kinematic conditions: $E_i = 16.6$ meV, $\theta_i = 31.9°$, $T_{crystal} = 80$ K. (b) A zoomed-in view of the spectrum shown in (a). Note the absence of the $^1/_2$-order peaks that were visible in the C10 analogue.

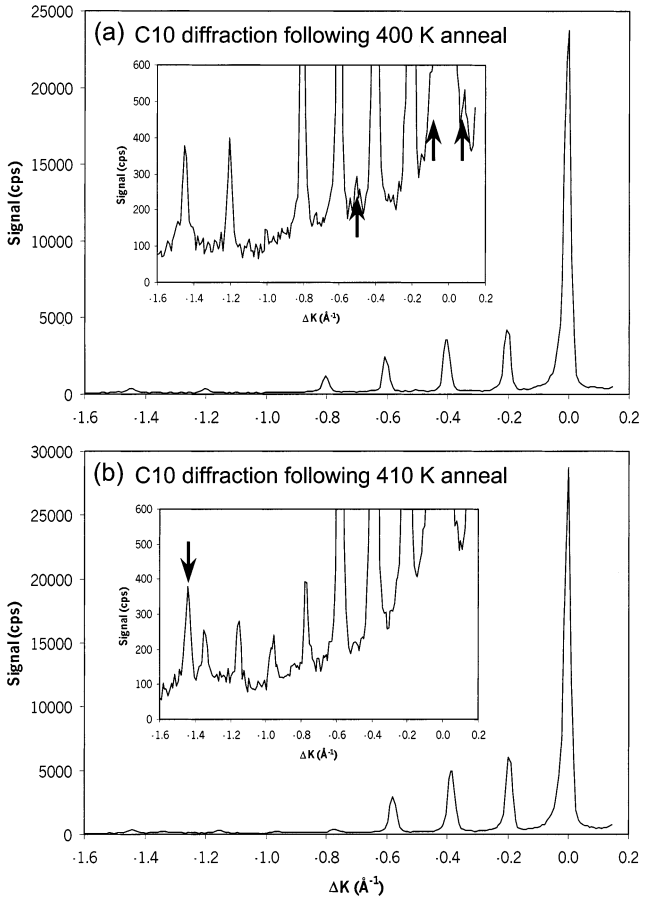

Figure 6. (a) Helium diffraction scan of 1-decanethiol on Au(111) in the ⟨110⟩ direction following a 10 min 400 K anneal. Seven subspecular orders of diffraction are observed. Kinematic conditions: $E_i = 16.6$ meV, $\theta_i = 36.9°$, $T_{crystal} = 80$ K. (b) Same system as in (a) after a 10 min 410 K anneal. Note the absence of the $^1/_2$-order peaks that were visible in (a), the contraction of the peak-to-peak spacing, and the appearance of the $\sqrt{3}$ peak at $\Delta K = -1.45$ Å^{-1}.

of C8 dimers without an awkward gap between them. A diffraction scan of the chemisorbed striped phase of C8/Au(111) showing four orders of diffraction is shown in Figure 5. As with C10, an average domain size of at least 400 Å is inferred from the width of the diffraction peaks. The peak-to-peak spacing in this spectrum is 0.228 Å^{-1}, implying either a (9.5 × $\sqrt{3}$) or a (10 × $\sqrt{3}$) unit cell depending on the reconstruction status of the substrate. This agrees with published STM data.[41] In contrast to the C10 spectrum, there is no evidence for $^1/_2$-order peaks between the principal diffraction peaks. Note, however, that this result does not imply that the surface is deconstructed. Even with a reconstructed substrate, the periodicity of this SAM does not coincide with the reconstruction and will therefore adopt a random relationship with the stacking fault transitions. This negative result does, nonetheless, illustrate that the $^1/_2$-order peaks are not a simple byproduct of alkanethiol striped phase structure. C10, due to its convenient dimension, serves as a window to the (usually hidden) substrate below. The presence of $^1/_2$-order peaks in the C10 diffraction spectrum is strongly redolent of substrate reconstruction. We note that $^1/_2$-order peaks have been observed by Camillone et al. in spectra of C6 striped phase SAMs.[32] This peak spacing indicates a periodicity of 45.6 Å; this spacing does not correspond to a simple integer fraction of the (23 × $\sqrt{3}$) reconstruction unit cell. A possible source for these peaks is a modified reconstruction that accommodates the molecular spacing of C6.

Assuming the substrate retains the reconstruction upon formation of the striped phase, the issue of its thermodynamic stability arises. That is, one wonders whether the herringbone structure is merely a metastable configuration when covered with a low-density thiol overlayer. There are two straightforward approaches to deconvoluting kinetic factors from the system: thermal annealing and varying the dosing rate. Multiple step-annealing experiments were performed in which the sample was annealed to progressively warmer temperatures (held at elevated temperature for 10 min) punctuated by quenches to 80 K in order to obtain structural information via helium diffraction. The typical temperature step sizes were 20 K in the range 280−380 K and 10 K in the range 380−430 K; the desorption temperature for chemisorbed C10 is approximately 415 K. Following anneals as high as 400 K, the $^1/_2$-order peaks were consistently still apparent, suggesting that the reconstruction is indeed thermodynamically stable despite the presence of the thiol overlayer. However, diffraction observed subsequent to annealing ≥410 K showed no evidence of fractional order peaks (Figure 6b). Moreover, the principal peak spacing uniformly contracted from 0.198 to 0.189 Å^{-1}, indicating

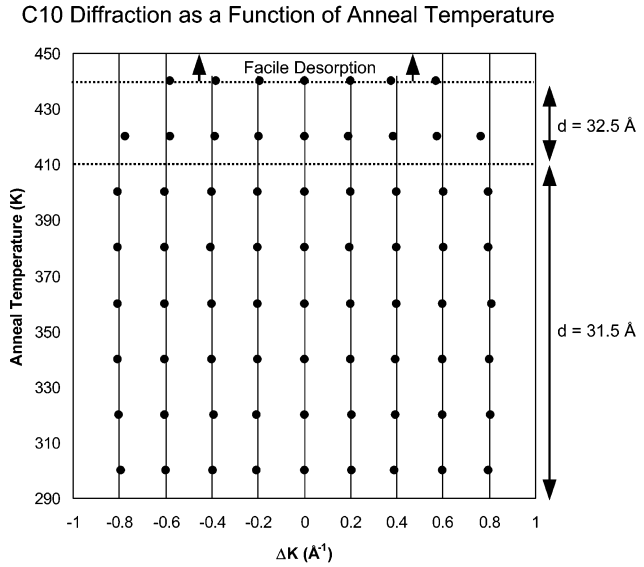

Figure 7. Plot of striped phase C10 diffraction peak positions in the ⟨110⟩ direction as a function of annealing temperature. Data are taken at a surface temperature of 80 K, regardless of the temperature of the anneal. Note the uniform contraction of the peak spacing when the anneal temperature is above 400 K.

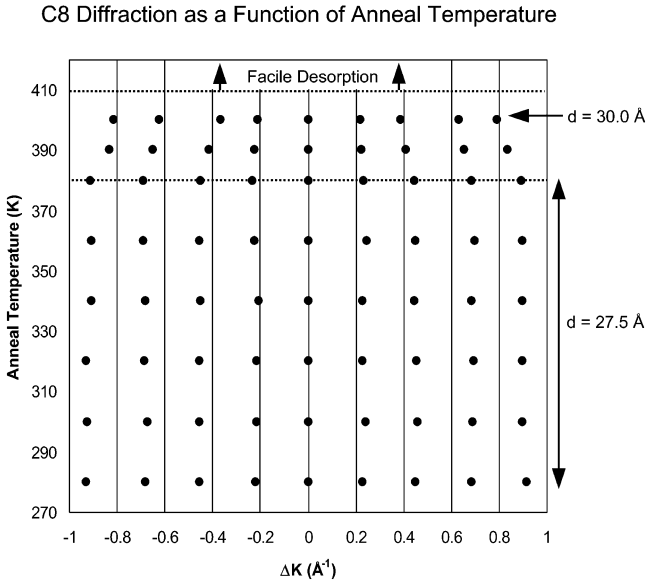

Figure 8. Plot of striped phase C8 diffraction peak positions in the ⟨110⟩ direction as a function of annealing temperature. Data are taken at a surface temperature of 80 K, regardless of the temperature of the anneal. Note the uniform contraction of the peak spacing when the anneal temperature is above 380 K. The data set at 390 K represents a transition region, and the set at 400 K represents the final state peak spacing.

an irreversible structural transformation in which the unit cell expands by roughly 4%. Figure 7 illustrates the SAM restructuring process by plotting the diffraction peak positions as a function of the annealing temperature. There is a clear trend of narrowing of the peak-to-peak distance following anneals near the desorption temperature.

The exclusive surface sensitivity of helium scattering prohibits direct observation of the underlying substrate, so it is unclear whether deconstruction occurs following this relatively high-temperature anneal. Regardless, the overlayer transformation is significant in itself and is well-suited to study via helium diffraction. Given the temperature of the shift-inducing anneal, the influence of thiol desorption must be considered; that is, the system must be regarded as being open. Analyzing the diffraction peak widths reveals no perceptible change in the size of the striped phase domains, although these widths are limited by the instrument function. One source of the unit cell shift could be straightforward partial desorption leading to a relaxation of the striped phase as it assimilates the surface area freed by the desorbing molecules. Another possible origin of the shift emerges when one looks further away from the specular angle (Figure 6b): a new peak has shown up in the postshift scan at $\Delta K = -1.45$ Å^{-1}, corresponding to $\sqrt{3}$ times the Au nearest-neighbor spacing. This peak is characteristic of the well-known standing phase of alkanethiol SAMs. Perhaps, therefore, the relaxation of the striped phase is enabled by a partial transformation to the higher density standing phase, conceivably in concert with partial desorption. This relaxation may also be associated with merging of neighboring domains. For completeness, Figure 8 shows a similar unit cell shift for the striped phase of C8.

A second kinetic factor is the rate at which C10 is dosed to the surface. If, for example, the dosing rate were extremely fast, it is conceivable that the substrate would not have sufficient time to deconstruct before being pinned in place by ordered, pinstriped thiol. Comparative experiments using a high-precision leak valve to extend the time required to obtain an exposure equivalent to that obtained with the directed doser produced results identical to those described above. One concludes, then, that the substrate is free to adopt the lowest energy configuration available during striped phase SAM growth.

To complement the reciprocal-space studies, STM experiments were also performed on the C10/Au(111) pinstripe system. Particular attention was paid to the initial stages of monolayer growth to allow for simultaneous imaging of the SAM and the substrate. Before exposure to C10, the gold crystal displayed expansive domains exhibiting both the $(23 \times \sqrt{3})$ and herringbone reconstructions (Figure 9a). Figure 9 depicts a series of images obtained following progressively larger exposures of C10, beginning with a clean substrate (a related experiment is described in ref 28). As observed by Poirier, the bright parallel lines indicative of the $(23 \times \sqrt{3})$ reconstruction stacking fault dislocations are clearly visible on those areas of the surface not directly covered with striped phase decanethiol. The herringbone periodicity in which the parallel lines zigzag on a scale of 250 Å *is* affected by alkanethiol adsorption (and, interestingly, vice versa), but the $(23 \times \sqrt{3})$ structure endures throughout. Indeed, $(23 \times \sqrt{3})$ bright parallel lines are discernible immediately adjacent to the growing C10 islands. Furthermore, no vacancy islands are observed on the gold surface. Vacancy islands have been shown to accompany deconstruction of the $(23 \times \sqrt{3})$ superlattice,[27] so their absence casts doubt on destruction of this reconstruction. We note that pits have been observed to exist simultaneously with the pinstripe phase of mercaptohexanol adsorbed on gold,[26] but none were observed in the course of the experiments described here. Indeed vacancy islands are only observed in association with the denser standing phase. These results agree well with the helium diffraction data presented above.

Conclusions

We have presented results from complementary real- and reciprocal-space experiments that mutually comprise compelling evidence for the persistence of the $(23 \times \sqrt{3})$ gold reconstruction following adsorption of a striped phase alkanethiol SAM. Measurements of the peak spacing in

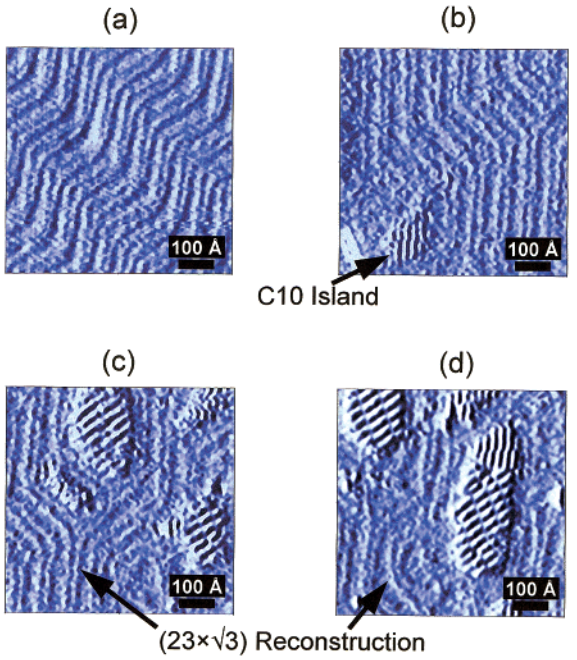

Figure 9. 600 Å × 600 Å STM images of (a) clean, reconstructed Au(111) surface exposed to progressively larger exposures of decanethiol: (b) 1, (c) 3, and (d) 5 langmuirs. The growing islands are composed of the well-known (11.5 × √3) striped phase. Experimental conditions: $T_{surface}$ = 298 K, 1 nA tunneling current, and +600 mV bias with respect to the tip.

helium diffraction spectra, when viewed in the context of the correct unit cell description, imply a substrate nearest-neighbor spacing corresponding to the compressed, reconstructed surface. The observed peak spacing is 0.198 Å^{-1}. Assuming a (11.5 × √3) unit cell, this spacing resolves the substrate nearest-neighbor spacing to be 2.76 Å—the correct spacing for the (23 × √3) reconstructed surface. Furthermore, a set of $^1/_2$-order peaks are observed, as a consequence of the coincidental length of the decanethiol molecule, which correspond to a repeat distance equivalent to the reconstructed unit cell dimension (63.4 Å). Two possible explanations for these additional peaks are (1) the substrate is still reconstructed or (2) neighboring dimers within alkanethiol striped phase SAMs are inherently distinct. The fact that no $^1/_2$-order peaks are observed in diffraction from striped phase octanethiol precludes the latter.

In agreement with previous work by Poirier, STM imaging of partial coverage striped phase monolayers also exhibit clear (23 × √3) reconstruction of the gold in those areas not obscured by thiolates. Moreover, no vacancy islands, which are connected with deconstruction, are observed. Fitts et al. recently proposed a heretofore unobserved rippling of gold atoms that would accommodate the excess atoms expelled during deconstruction.[29] In light of the new results presented here, there is no need to invoke an atomic rippling because the persistent reconstruction explains all of the real- and reciprocal-space observations. Together, these results refute the common hypothesis that deconstruction necessarily follows formation of a thiolate SAM.

Acknowledgment. The authors thank Paul Fenter, Peter Schwartz, and Giacinto Scoles for calling to our attention two Princeton theses (refs 30 and 40) and unpublished X-ray data relevant to this study. The authors also thank Kenneth Nicholson for helpful discussions. The STM experiments were primarily supported by the Chemical Sciences, Geosciences and Biosciences Division, Office of Basic Energy Sciences, Office of Science, U.S. Department of Energy, Grant DE-FG02-00ER15089. This work was also supported by the NSF-MRSEC at the University of Chicago Award DMR-9808595.

LA020334X